Acta Oceanol. Sin., 2018, Vol. 37, No. 1, P. 108–114
DOI: 10.1007/s13131-018-1161-0
http://www.hyxb.org.cn
E-mail: hyxbe@263.net

Wave height estimation using the singular peaks in the sea echoes of high frequency radar

ZHOU Hao[1]*, WEN Biyang[1]

[1] School of Electronic Information, Wuhan University, Wuhan 430072, China

Received 7 November 2016; accepted 21 February 2017

Abstract

The popular methods to estimate wave height with high-frequency (HF) radar depend on the integration over the second-order spectral region and thus may come under from even not strong external interference. To improve the accuracy and increase the valid detection range of the wave height measurement, particularly by the small-aperture radar, it is turned to singular peaks which often exceed the power of other frequency components. The power of three kinds of singular peaks, i.e., those around ±1, $\pm\sqrt{2}$ and $\pm 1\sqrt{2}$ times the Bragg frequency, are retrieved from a one-month-long radar data set collected by an ocean state monitoring and analyzing radar, model S (OSMAR-S), and *in situ* buoy records are used to make some comparisons. The power response to a wave height is found to be described with a new model quite well, by which obvious improvement on the wave height estimation is achieved. With the buoy measurements as reference, a correlation coefficient is increased to 0.90 and a root mean square error (RMSE) is decreased to 0.35 m at the range of 7.5 km compared with the results by the second-order method. The further analysis of the fitting performance across range suggests that the $\sqrt{2}$ peak has the best fit and maintains a good performance as far as 40 km. The correlation coefficient is 0.78 and the RMSE is 0.62 m at 40 km. These results show the effectiveness of the new empirical method, which opens a new way for the wave height estimation with the HF radar.

Key words: high frequency radar, wave height, Bragg peak, singular peak, ocean state monitoring and analyzing radar

Citation: Zhou Hao, Wen Biyang. 2018. Wave height estimation using the singular peaks in the sea echoes of high frequency radar. Acta Oceanologica Sinica, 37(1): 108–114, doi: 10.1007/s13131-018-1161-0

1 Introduction

The high frequency (HF) radar has now been widely used as an efficient tool to monitor the sea surface states such as the surface current velocity, wave height, and wind direction. The echo Doppler spectrum from the sea surface is dominated by two strong peaks due to the first-order Bragg scattering and the surrounding weaker second-order side-bands. On the basis of the existing first-and second-order radar cross-section (RCS) equations, firstly proposed by Barrick(1972, 1977), and later improved by Gill et al. (2006), the echo Doppler spectrum is related to the directional wave spectrum and consequently the information on the current, wave and wind can be extracted from the Doppler spectrum. The surface current velocity can be easily estimated from the Doppler shift of the first-order Bragg peak using the dispersion relation, and thus it has been developed into an important product. However, the estimation of the wave height, and further the wind speed, is still somewhat a challenge, which relies on a much more complex integral inversion of the second-order spectrum. Although the theoretical framework for the interpretation and inversion of the second-order spectrum is nearly perfect and has achieved success in a series of HF radar experiments (Heron and Prytz, 2002; Wyatt et al., 2003; Lipa and Nyden, 2005; Long et al., 2011; Hisaki, 2014; Toro et al., 2015; Zhou et al., 2015), there are still some issues that should be resolved in the wave height inversion. First, the second-order spectral continuum is generally much weaker than the first-order peaks and has a low signal-to-noise power ratio (SNR), so the wave height estimate is susceptible to the external noise. This is also a main reason why the detection range of the wave height is far less than the current. Second, in a small-aperture radar with large receive beam-width, the spatial aliasing of the first- and second-order spectra can lead to big error, particularly when the current velocity has a complex distribution. Moreover, in the second-order spectral region, there also exist some singular peaks other than the continuum. These singular peaks result from particular wave components and may far exceed those from other wave components, particularly under a low or medium sea state, which may also introduce error into the wave height estimation. Consequently, there is a big gap between the performances of the wave height and current estimation in both the accuracy and detection range. The situation is even worse in small-aperture radars due to the lack of a high spatial gain. Because many marine applications focus on the wave and wind information, the study of the wave height estimation method is still a must. We want to explore other ways to perform the calculation of the significant wave height (SWH) taking into account the values of the second-order spectrum at some particular frequencies.

Since the singular peaks often exceed the continuum in the echo Doppler spectrum under a low or medium sea state, we turn to reexamine their power response to the wave height.

Foundation item: The National Natural Science Foundation of China under contract No. 61371198; the National Special Program for Key Scientific Instrument and Equipment Development of China under contract No. 2013YQ160793.
*Corresponding author, E-mail: zhou.h@whu.edu.cn

Among the singular peaks, there are the first-order peaks and the second-order peaks, including the second harmonic peaks and the corner reflection peaks. These second-order peaks were extensively studied by Lipa and Barrick (1986) and Ivonin et al. (2006), where they were modelled as echoes scattered from two coupled sea waves. However, other singular peaks have also been observed in our radar spectra, e.g., the peaks near $\pm 1/\sqrt{2}$ times the standard Bragg frequency, which cannot be readily explained by the classical theory. They may be due to the non-Bragg scattering from the sea wave with a wavelength being equal to that of the radar (Wen and Li, 2016), a more detailed explanation will be part of our future work. It is observed from our experimental data (Zhou et al., 2015) that, the peaks near $\pm\sqrt{2}$ and $\pm 1/\sqrt{2}$ are two kinds of strong peaks in the second-order region, while the corner reflection peaks are quite small and thus can be neglected. Moreover, the direct relationship between their strengths and the SWH has not been fully studied yet. In the conventional methods for the SWH estimation, an integral over the second-order region is involved. Small weights are assigned to these singular peaks (Barrick, 1977), which essentially decreases their impact on the final results. However, if we look into them from another perspective, they will become beneficial and some useful results can be achieved.

According to the first-order radar cross-section equation, a Bragg peak is related to a single sea wave, which wavelength is half of the radio wave, and the strengths of the first-order Bragg peaks are proportional to the directional wave spectral values at the Bragg frequency. The Bragg peak contains good information of the wave height below the saturation limit, but it is only used as a normalization factor to linearize the second-order equation in the conventional wave height estimation method (Barrick, 1977; Howell and Walsh, 1993). Encouragingly, some researchers have noticed the relationship between the strengths of the singular peaks and the SWH and achieved some progress recently. Zhou and Wen (2014) observed that the second harmonic peak was also mainly related to a single sea wave, with its wavelength being equal to that of the radar, and found the power ratio of the second harmonic peak to the Bragg peak to be a good index for the wave height estimation. Furthermore, Zhou and Wen (2015) directly fitted the power response of the Bragg peak to a nonlinear model and achieved better wave height estimates than those given by the conventional second-order method under a low or moderate sea state. These studies have opened a wider use of both the first- and second-order singular peaks. In this paper, we further analyzed the power response of the singular peaks to the wave height based on a one-month-long data set collected by the HF radar OSMAR-S, and found that they complied with a two-parameter nonlinear model quite well.

2 Radar experiment

The HF radar used in this study is the OSMAR-S developed by Wuhan University of China, whose performances on the measurements of the current and the wave height have been validated by several experiments (Wen et al., 2009; Zhou et al., 2015). From January to March of 2013, a radar was deployed on the Fujian coast to measure the surface sea states in the Taiwan Strait. Figure 1 shows the map of the experiment, the positions of the radar site and the wave buoys used for comparison, and the bathymetric contour lines in that area. The radar worked near 13 MHz with a bandwidth of 60 kHz, employing a compact antenna system, say, a whip transmit antenna and a cross-loop/monopole receive antenna. The two wave buoys used in this study, namely A and C, were deployed 44.0 and 10.5 km away from the radar, respectively, and both positions satisfied the deep-water condition with respect to the radar wavelength. Wave and wind parameters were provided by the buoys every hour for comparison with the radar measurements. In this paper the data set in February was used to study on the singular peaks. During this period, the wind speed and the wave height experienced a series of wind events, which are shown in Fig. 2. As measured by Buoy A, the wind predominantly blew from the northeast subject to the strait direction and the speed varied from 0 to about 18 m/s, and the SWH varied from 0 to about 4.4 m correspondingly. The nearly constant winds made the waves develop in a manner almost similar and have similar wave heights at Buoys A and C. The wave heights at

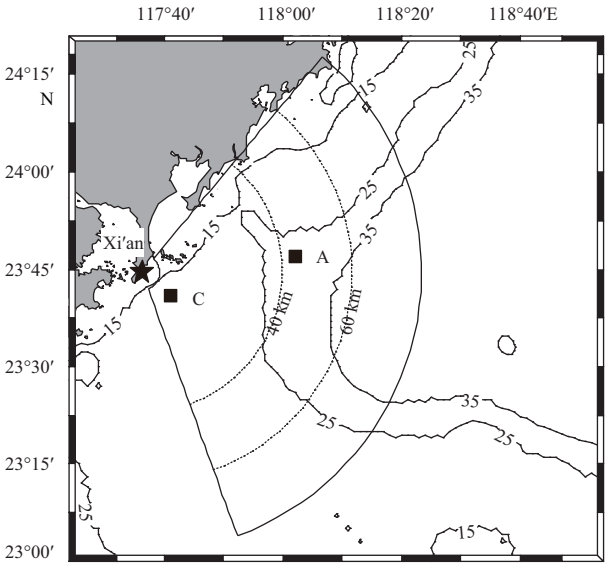

Fig. 1. Radar coverage area of the HF radar system deployed during the OSMAR-S experiment in the Taiwan Strait in 2013. Bathymetric contour (m) lines are also shown. The radar site Xi'an is marked by a pentagon and the wave buoys, namely A and C, are marked by squares. Radar coverage area is delimited with a black line.

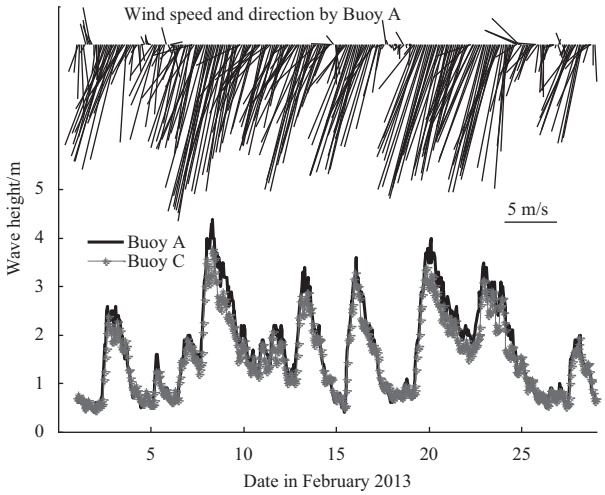

Fig. 2. Buoy-measured wind speed, direction (to) and wave height in February 2013. The SWHs measured by Buoys A and C are plotted simultaneously, whereas only the wind vectors measured by Buoy A are shown for clarity.

Buoy C had a small time lag to those at Buoy A, and the values at Buoy C were generally about 0.83 times those at Buoy A, which is in accordance with the relativity of the wind speeds.

3 Modeling and estimation

3.1 *Theoretical basis*

According to the first-order RCS equation the power response of the Bragg peak, $\sigma(\omega,\varphi)$, is proportional to the directional wave spectrum, $S(\omega,\varphi)$, which can be denoted as

$$\sigma(\omega,\varphi)=Y(\omega)S(\omega,\varphi), \tag{1}$$

where ω is the angular frequency, φ is the radar look angle, and $Y(\omega)$ is the transfer function.

The directional wave spectrum $S(\omega,\varphi)$ can be modeled as the product of the non-directional wave height spectrum $F(\omega)$ and the wave directional spreading function $G(\varphi-\theta)$, that is,

$$S(\omega,\varphi)=F(\omega)G(\varphi-\theta), \tag{2}$$

with θ being the wind direction. The SWH can be calculated by the non-directional wave spectrum via $H_S=4\sqrt{\int_0^\infty F(\omega)\mathrm{d}\omega}$. The wind directional spreading function is symmetric about 0, with its maximum and minimum values locating at 0 and π, respectively. Without loss of generality, we assume $G(0)=1$.

3.2 *Preprocessing*

The radar data set consists of a series of range-Doppler spectra with each obtained in a period of about 6.5 min. The size of the range cell is 2.5 km. An example of a Doppler spectrum under a moderate wave height is shown in Fig. 3. Here for brevity the abscissa is set to be the Doppler frequency (f_D) normalized to the Bragg frequency f_B, which is determined by the radar frequency f_0, that is,

$$f_B=\sqrt{\frac{gf_0}{2\pi c}}, \tag{3}$$

where g is the gravity acceleration; and $\pm\sqrt{2}$ is the speed of the light. As can be seen, there are strong peaks around and $\pm1/\sqrt{2}$ as well as ±1, which exceed the surrounding spectral components. The peaks on the positive and negative sides are respectively generated by the sea waves approaching and receding the radar, and their offsets from the corresponding standard frequencies are due to the underlying surface currents.

Before we proceeded to study the relationship between the strengths of the singular peaks and the wave height, a preprocessing program was executed. Because the OSMAR-S uses a broad beam for receive, the Doppler spectrum is a superposition of sea echoes from the same range but different azimuths. The singular peaks often spread and split onto a number of frequency bins due to the nonuniform distribution of radial current velocities. Consequently, there are a number of groups of singular peaks with each having nearly the same Doppler shift, and their positions are slowly time-variant due to the fluctuation of the currents. So, the Doppler shifts of the singular peaks should be compensated to guarantee that the same wave group is tracked. Moreover, the echoes from different azimuths involve

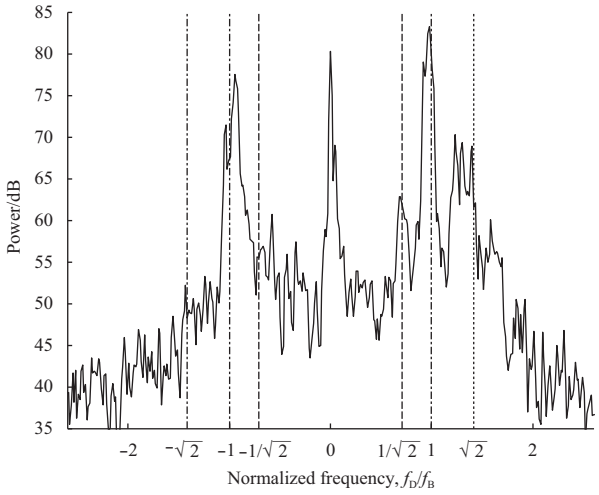

Fig. 3. Doppler spectrum at the range of 7.5 km with the SWH 2 m at 02:02:14 on February 3, 2013.

different wave direction spectra, which so far are hard to model well due to the insufficient angular resolution of this radar. To avoid this important uncertainty, we simply tracked the singular spectral group corresponding to the maximum Bragg peak on the side of positive Bragg frequency. As a result, all the Doppler spectra at a given range cell were aligned with the maximum Bragg peaks being located at the normalized Bragg frequency +1, simultaneously removing the two adverse impacts mentioned above. Here the Doppler spectra were firstly calculated on 6.5 min intervals of the coherent integration time (CIT) and then averaged every hour. The aligned positive-side spectra at the range cell of 7.5 km during the experiment are shown in Fig. 4a, from which we can see that the overall spectral power varies in accordance with the wave height as shown in Fig. 2 and that there are three characteristic spectral regions in the intervals of [0.9, 1.1], [1.3, 1.5], and [0.7, 0.8], respectively. The radar power sequence at the normalized frequency of $\sqrt{2}$ in comparison with the SWH measured by Buoy C is shown in Fig. 4b. Thus, the power sequences at each frequency can be read out directly and averaged hourly onto the same time grid as the buoy for further analysis. Because the Doppler spectra have the highest SNR at the first valid range cell, say 7.5 km, and the sea surface states are almost the same within a small area, hereinafter the Doppler spectra at 7.5 km are used for modeling unless otherwise specified.

3.3 *Empirical model*

With the help of the *in situ* wave buoys, we were able to model the power response of a wave component to the wave height. The powers of the singular peaks at 1, $\sqrt{2}$ and $1/\sqrt{2}$ are plotted in Fig. 5, respectively. As can be seen, they exhibit similar distributions with initial monotonic increase and then saturation at the wave heights depending on the sea wavelengths corresponding to the singular peaks respectively. We found that the power complies with a simple model quite well, which is given by

$$\sigma_{\mathrm{dB}}(\omega)=10\log_{10}\sigma(\omega)=\alpha(\omega)+\beta(\omega)H_s^{0.4}, \tag{4}$$

where $\alpha(\omega)$ and $\beta(\omega)$ are two frequency-dependent coefficients. Linear fitting was performed to determine $\alpha(\omega)$ and $\beta(\omega)$ for each type of singular peak respectively, and the results are shown

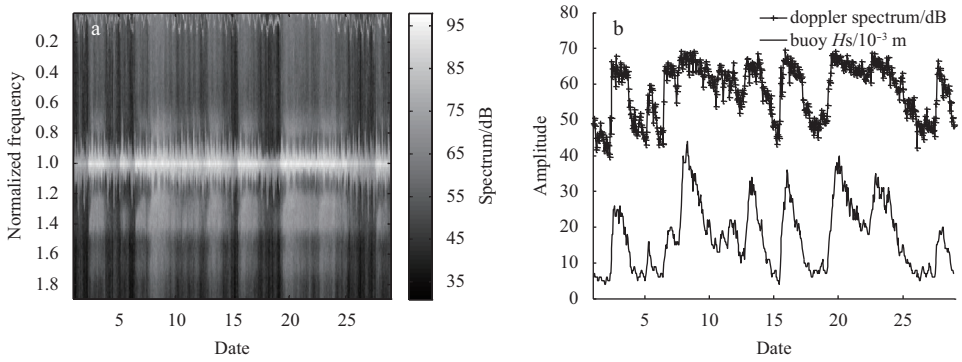

Fig. 4. Aligned Doppler spectra at 7.5 km in February 2013. a. Overall spectra, and b. time sequence of spectral values at $f_D/f_B = \sqrt{2}$ in comparison with the SWH measured by Buoy C. For clarity the wave height plotted has been multiplied by 10.

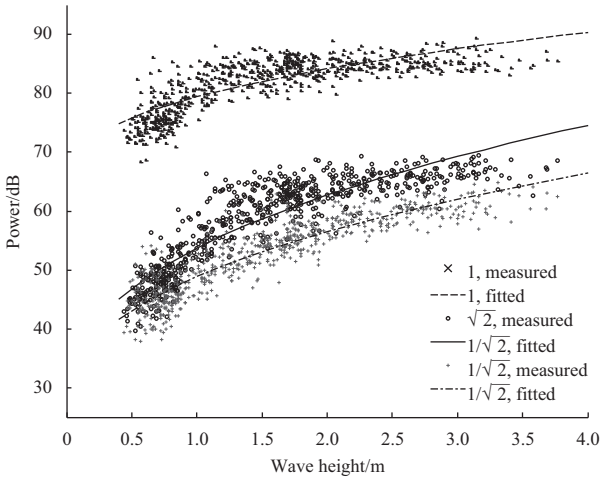

Fig. 5. Amplitude response of the singular peaks to the wave height using the Buoy C measurement as reference.

in Fig. 5. It should be pointed out that, the measured SWHs by Buoy C were between 0.4 and 3.8 m, and the empirical model here was solved within these limits without extrapolation.

3.4 *Estimation*

Using this model, the SWH can be estimated by the powers of the singular peaks, that is,

$$\hat{H}_S = \left[\frac{\sigma_{dB}(\omega)-\hat{\alpha}(\omega)}{\hat{\beta}(\omega)}\right]^{2.5}. \quad (5)$$

We further used this model to fit all the wave components within a range of 0.2 to 1.9 in the normalized frequency, corresponding to about 0.07 to 0.70 Hz at the 13 MHz band, and achieved the corresponding estimates of the SWH. The estimated values of $\hat{\alpha}(\omega)$ and $\hat{\beta}(\omega)$, and the root mean square error (RMSE) and the correlation coefficient of $\hat{H}_S$ are shown in Fig. 6, respectively. We can see that, the singular peaks all have very good model fit and strong response showing a high sensibility to the wave height. Although the $\sqrt{2}$ peak is generally 15 to 30 dB lower than the Bragg peak (Fig. 5), it shows a quite good fit to the wave height, with the correlation coefficient being high up to 0.88 and the RMSE down to 0.45 m. The Bragg peak has a less good fit, with the correlation coefficient 0.76 and the RMSE 0.66 m. The $1/\sqrt{2}$ peak shows the best fit with the correlation coefficient 0.91 and the RMSE 0.41 m. However, the susceptibility of the $1/\sqrt{2}$ peak to noise should be taken into consideration since it is still about 10 dB weaker than the $\sqrt{2}$ peak, and therefore the $\sqrt{2}$ peak and the Bragg peak should be better indices for the wave height estimation. To demonstrate more details, the scatter plots of the wave heights estimated via the three peaks versus the buoy measurements are shown in Fig. 7. The correlation coefficient and the RMSE as well as the 95% prediction intervals (PIs) of the fitting models are also shown in each subfigure respectively. As can be seen, when the wave height increases to be closer to the saturation limits, all the PIs become larger, leading to a lower accuracy of the wave height estimates. The PIs of the $\sqrt{2}$ and $1/\sqrt{2}$ peaks are similar, obviously smaller than those of the Bragg peak. The estimation performance has been improved compared with the results on the same data set via a semiempirical method reported by Zhou et al. (2015), where the correlation coefficient was 0.74 and the RMSE was 0.77 m. When compared with the results via the empirical model for the first-order Bragg peak reported by Zhou and Wen (2015), where the correlation coefficient was 0.78 and the RMSE was 0.59 m, the new model seems to be less good, but the saturation limit for the wave height estimation has been increased from about 3 m to above 3.5 m. This study has revealed some novel properties of the singular peaks, which opens a new way to estimate the wave height.

3.5 *Estimation at far range cells*

Because the singular peaks are generally much stronger than the spectral continuum, an increased detection range of the wave height can be expected. There is extra attenuation introduced to the echoes at the far range cells due to the propagation losses and the modulation of the radar's gating pulses, for which a simple way is to use a fixed $\beta(\omega)$ while a variable $\alpha(\omega)$ at each range cell respectively. It is noteworthy that the range equation can be determined once the radar waveform is given. In fact the model parameters only need to be calibrated at one range cell, and at other range cells $\alpha(\omega)$ can be calculated. Here for simplicity we neglect the additional propagation loss due to the Norton attenuation factor (Norton, 1937), which is less than 1 dB for 13 MHz when the range is less than 50 km. Thus, the model in Eq. (4) can be rewritten as

$$\sigma_{dB}(\omega,R) = 10\log_{10}\sigma(\omega,R) = \alpha(\omega,R) + \beta(\omega)H_s^{0.4}(R) \quad (6)$$

with R being the range, and the estimation Eq. (5) should be re-

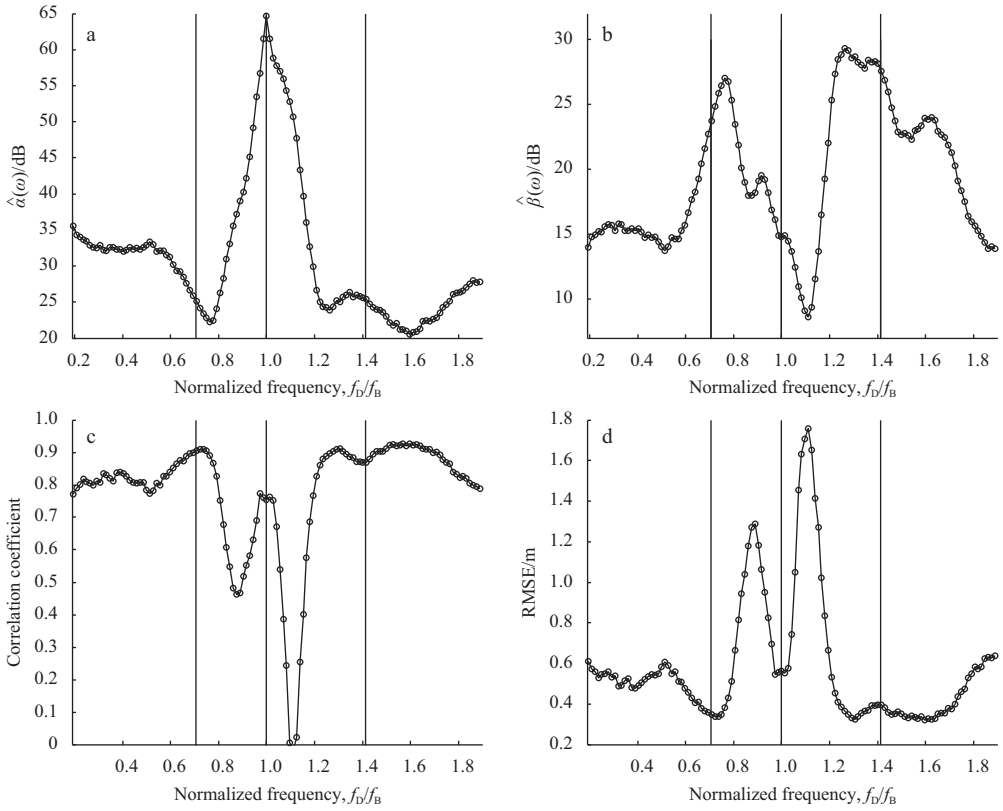

Fig. 6. Estimated model parameters at 7.5 km. a. $\sqrt{2}$, b. $\hat{\beta}(\omega)$, c. correlation coefficient and d. RMSE. The three vertical lines, from left to right, indicate the $1/\sqrt{2}$, Bragg, and $\sqrt{2}$ peaks, respectively.

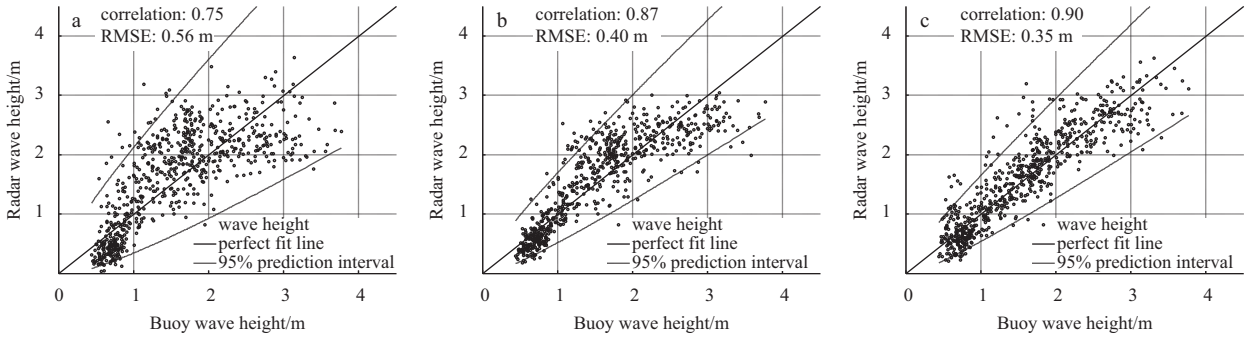

Fig. 7. Scatter plots of the SWH estimated by the singular peaks at 7.5 km versus that measured by Buoy C. a. The Bragg peak, b. the $\sqrt{2}$ peak and c. the $1/\sqrt{2}$.

vised accordingly. As mentioned before, the wave heights at Buoy C are generally 0.83 times of those at Buoy A and they varied almost similar, so either one can be used as reference for comparison. The estimation performance across the range cells using the measurements by Buoy C as reference is shown in Fig. 8. As can be seen, generally the $\sqrt{2}$ peak outperforms the other two peaks in both the correlation and the RMSE, and its performance degrades slowly within 40 km, where the correlation coefficient is 0.75 and the RMSE is 0.52 m. So, in this radar scenario we can expect a valid range of 40 km for the use of the $\sqrt{2}$ peak in the wave height estimation. Then, the wave height measured by Buoy A was used as reference to further test this far range estimation. The scatter plot of the wave height estimated by the $\sqrt{2}$ peak at 40 km versus the Buoy A measurement is shown in Fig. 9. General coincidence can be clearly seen, but the increase of the prediction interval is also obvious than that at 7.5 km due to the attenuated signal strength. This result is even better than that achieved by the conventional second-order method at 7.5 km, namely a correlation coefficient of 0.67 and a RMSE of 0.89 m, reported by Zhou et al. (2015).

4 Discussion

4.1 *Model generality*

Like other empirical method, the proposed method for the wave height estimation also need further test in a model generality. The key point of the proposed method is to estimate the SWH directly from the power of the singular peak, which is in fact a

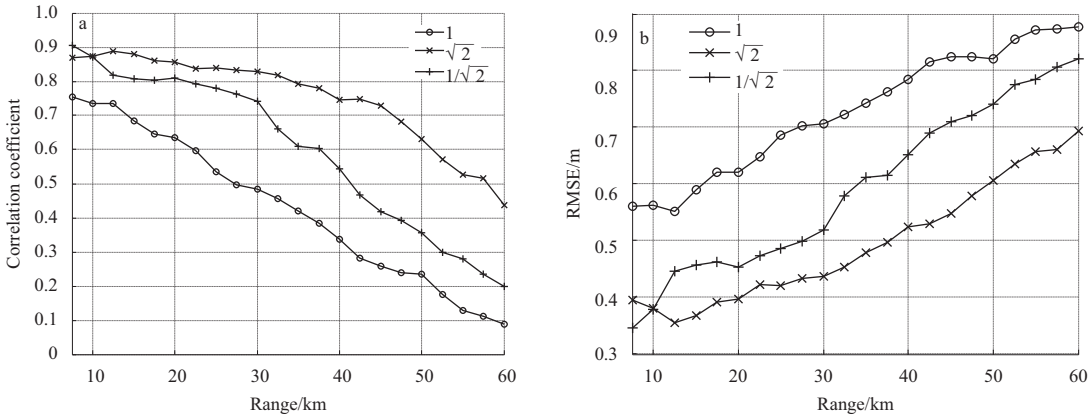

Fig. 8. Wave height estimation performances across range using measurement by Buoy C as reference. a. Correlation coefficient and b. RMSE.

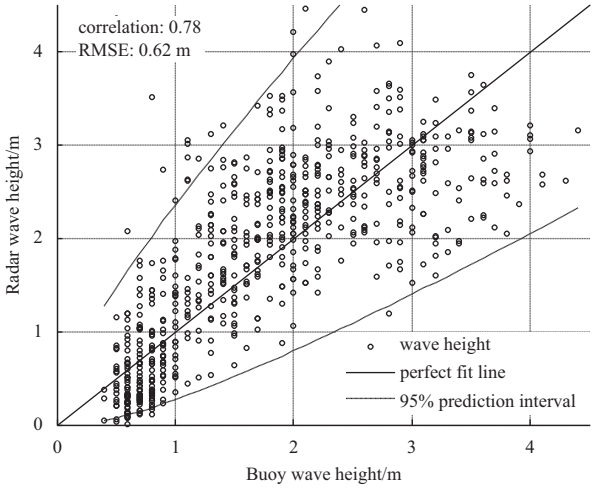

Fig. 9. Scatter plot of the SWH estimated by the $1/\sqrt{2}$ peak at 40 km versus that measured by Buoy A.

single sample of the wave height spectrum. The wave spectrum depends on a wind-sea evolution or swell presence and therefore the α and β coefficients should be calibrated at each location. However, for a particular radar system working in a particular sea area, such an empirical model is undoubtedly beneficial. The data measured by the radar HF in this experiment may have energy corresponding to swell and therefore this model can be used in places with presence of swell. Another issue is the form of the model itself. In this paper we used a rather simple model, which is also easy to solve and thus convenient for marine applications. There is still space for improvement on the model, and we will keep on studying it.

4.2 *Unsupervised estimation*

In the above estimation process, the model coefficients in Eq. (4), namely $\alpha(\omega)$ and $\beta(\omega)$, need to be determined in advance, where the *in situ* buoy is necessary. However, in many situations there may be no buoys available. In such circumstances, the wave height estimated by the conventional second-order method can be used as the "ground truth" data alternatively. As mentioned above, the second-order spectra are often susceptible to the external noise, so some data quality control measures should be taken. The methodologies to extract the second-order spectrum with sufficient SNR and properly (Hisaki, 2005; Wyatt et al., 2011; Toro et al., 2015) can be used to improve the final estimation performance.

4.3 Cancellation of system uncertainties

The strength of a singular peak includes some particular component of the wave spectrum and the total system gain. The total gain consists of the gain in the case of propagation in vacuum (including the gains of the transmitter, antenna, and the receiver) and the additional propagation loss over the sea surface. The wave height itself, or equivalently the sea surface roughness, is an important factor that influences the echo strength. This effect is included in the Norton attenuation factor, which depends on both the radar range and the sea state. In the lower HF band (3–10 MHz) and at close ranges (<10 km), the additional propagation loss can be neglected. However, in the upper HF band and at farther ranges, it becomes significant and thus make the estimation via a single singular peak invalid. To account for the system uncertainties, a good choice is to use the power ratio of the $\sqrt{2}$ peak (i.e., the second harmonic peak) to the Bragg peak in the estimation. The ratio was used by Zhou and Wen (2014), leading to obvious improvement on the wave height estimation compared with the conventional second-order method. A further improvement can be expected with the new model in this paper.

5 Conclusions

In this paper we proposed a new empirical model for the power response of the three kinds of singular peaks, say, the peaks at the normalized frequencies of 1, $\sqrt{2}$ and $1/\sqrt{2}$, to the wave height in the HF radar echo spectrum. Here only the spectral values at positive frequencies were explored, but the analysis is expected to be also suitable for negative frequencies in case that the negative side of the Doppler spectrum was more energetic. Generally the $\sqrt{2}$ peak has the best fit, which is expected to improve the estimation of the SWH below the saturated wave height limit. The correlation coefficient between the measurements of the radar and the buoy is 0.88 and the RMSE is 0.45 m at the range of 7.5 km. The fitting performance across the ranges also indicates that the $\sqrt{2}$ peak is the best index for the wave height estimation under the proposed model. In the radar scenario involved, the $\sqrt{2}$ peak can be used to estimate the wave height at a range far to 40 km, with the correlation coefficient be-

ing above 0.78 and the RMSE 0.62 m. This study revealed some new properties of the singular peaks and provided a new way for the wave height estimation. However, there is still space for further improvement on the model for the power response of the singular peaks, and steps of interference suppression and data quality control should also be carried out to eliminate the outliers in the wave height estimates. These will be included as part of our future work. Furthermore, we will test the model under different radar frequencies to make it more reliable for operational use.

Acknowledgements

The authors thank the personnel of Wuhan Device Electronic Technology Co., Ltd for carrying out the radar experiment, and thank Shang Shaoping of Xiamen University for providing the buoy data.

References

Barrick D E. 1972. First-order theory and analysis of MF/HF/VHF scatter from the sea. IEEE Transactions on Antennas and Propagation, 20(1): 2–10

Barrick D E. 1977. Extraction of wave parameters from measured HF radar sea-echo Doppler spectra. Radio Science, 12(3): 415–424

Gill E, Huang Weimin, Walsh J. 2006. On the development of a second-order bistatic radar cross section of the ocean surface: a high-frequency result for a finite scattering patch. IEEE Journal of Oceanic Engineering, 31(4): 740–750

Heron M L, Prytz A. 2002. Wave height and wind direction from the HF coastal ocean surface radar. Canadian Journal of Remote Sensing, 28(3): 385–393

Hisaki Y. 2005. Ocean wave directional spectra estimation from an HF ocean radar with a single antenna array: observation. Journal of Geophysical Research: Oceans, 110: C11004

Hisaki Y. 2014. Inter-comparison of wave data obtained from single high-frequency radar, *in situ* observation, and model prediction. International Journal of Remote Sensing, 35(10): 3459–3481

Howell R, Walsh J. 1993. Measurement of ocean wave spectra using narrow-beam HE radar. IEEE Journal of Oceanic Engineering, 18(3): 296–305

Ivonin D V, Shrira V, Broche P. 2006. On the singular nature of the second-order peaks in HF radar sea echo. IEEE Journal of Oceanic Engineering, 31(4): 751–767

Lipa B J, Barrick D E. 1986. Extraction of sea state from HF radar sea echo: mathematical theory and modeling. Radio Science, 21(1): 81–100

Lipa B, Nyden B. 2005. Directional wave information from the SeaSonde. IEEE Journal of Oceanic Engineering, 30(1): 221–231

Long R M, Barrick D, Largier J L, et al. 2011. Wave observations from Central California: SeaSonde systems and in situ wave buoys. Journal of Sensors, 2011: 728936

Norton K A. 1937. The propagation of radio waves over the surface of the earth and in the upper atmosphere. Proceedings of the Institute of Radio Engineers, 25(9): 1203–1236

Toro V G, Ocampo-Torres F J, Osuna P, et al. 2015. Analysis of fetch-limited wave growth using high-frequency radars in the gulf of Tehuantepec. Ciencias Marinas, 40(2): 113–132

Wen Biyang, Li Ke. 2016. Frequency shift of the Bragg and non-Bragg backscattering from periodic water wave. Scientific Report, 6: 31588

Wen Biyang, Li Zili, Zhou Hao, et al. 2009. Sea surface currents detection at the Eastern China Sea by HF ground wave radar OSMAR-S. Acta Electronica Sinica (in Chinese), 37(12): 2778–2782

Wyatt L R, Green J J, Gurgel K W, et al. 2003. Validation and intercomparisons of wave measurements and models during the EuroROSE experiments. Coastal Engineering, 48(1): 1–28

Wyatt L R, Green J J, Middleditch A. 2011. HF radar data quality requirements for wave measurement. Coastal Engineering, 58(4): 327–336

Zhou Hao, Roarty H, Wen Biyang. 2015. Wave height measurement in the Taiwan Strait with a portable high frequency surface wave radar. Acta Oceanologica Sinica, 34(1): 73–78

Zhou Hao, Wen Biyang. 2014. Observations of the second-harmonic peaks from the sea surface with high-frequency radars. IEEE Geoscience and Remote Sensing Letters, 11(10): 1682–1686

Zhou Hao, Wen Biyang. 2015. Wave height extraction from the first-order Bragg peaks in high-frequency radars. IEEE Geoscience and Remote Sensing Letters, 12(11): 2296–2300